



Carbon dioxide capture capacity of sodium hydroxide aqueous solution

Miran Yoo, Sang-Jun Han, Jung-Ho Wee*

Department of Environmental Engineering, The Catholic University of Korea, 43 Jibong-ro, Wonmi-gu, Bucheon-si, Gyeonggi-do 420-743, Republic of Korea

ARTICLE INFO

Article history:

Received 19 October 2011

Received in revised form

19 September 2012

Accepted 3 October 2012

Available online 24 November 2012

Keywords:

Climate change

Carbon capture

Chemical absorption

Greenhouse gas

Absorbent

Sodium hydroxide

ABSTRACT

The present paper investigates the various features of NaOH aqueous solution when applied as an absorbent to capture carbon dioxide (CO₂) emitted with relatively high concentration in the flue gas. The overall CO₂ absorption reaction was carried out according to consecutive reaction steps that are generated in the order of Na₂CO₃ and NaHCO₃. The reaction rate and capture efficiency were strongly dependent on the NaOH concentration in the Na₂CO₃ production range, but were constant in the NaHCO₃ production step, irrespective of the NaOH concentration. The amount of CO₂ absorbed in the solution was slightly less than the theoretical value, which was ascribed to the low trona production during the reaction and the consequent decrease in CO₂ absorption in the NaOH solution. The mass ratio of absorbed CO₂ that participated in the Na₂CO₃, NaHCO₃, and trona production reactions was calculated to be 20:17:1, respectively.

© 2012 Elsevier Ltd. All rights reserved.

1. Introduction

Among the greenhouse gases, carbon dioxide (CO₂) is the most influential gas on global warming (Gangopadhyay et al., 2008; Zhao et al., 2006). The use of fossil fuels has drastically increased since the Industrial Revolution and has greatly increased CO₂ emissions to the atmosphere. Therefore, the world currently faces climate change and many nations have made a great effort to reduce CO₂ emissions (Heitmann and Khalilian, 2011).

Carbon capture and storage (CCS) is believed to be a promising technology to reduce CO₂ emissions (Gerard and Wilson, 2009). With various CCS technologies, the use of fossil fuels, particularly coal, which is relatively cheap and abundant, will continue while CO₂ emissions are substantially reduced.

Chemical absorption of CO₂ into amine-based solvents such as mono-ethanol-amine (MEA) is a capture process that is currently adopted as almost the only commercialized process in most post-combustion plants. However, MEA must be regularly topped up due to loss arising from its high volatility and the solvent degradation (Nguyen et al., 2010) that occurs in the process. In addition, the solvent is a highly corrosive substance and a lot of energy is required for MEA recovery (Leifsen, 2007; Zhao et al., 2011; Qin et al., 2010; Kittel et al., 2009).

CO₂ can also be captured by absorbing it into NaOH aqueous solutions (Stolaroff et al., 2008). In fact, the CO₂ absorption capacity of NaOH solution is higher than that of MEA. The theoretical amount of MEA and NaOH to capture a ton of CO₂ is 1.39 and 0.9 tons, respectively. In addition, NaOH is even more abundant, cheaper and more familiar than MEA.

CO₂ absorption in NaOH solution has been studied extensively since the 1940s (Tepe and Dodge, 1943; Spector and Dodge, 1946). However, the papers at that time did not aim to reduce CO₂ emission with respect to global climate change. Most of them mainly focused on purely academic endeavors such as finding the mass transfer coefficient, absorption rate, film resistance and performance of the system, which includes scrubber and packing material. This topic continues to be explored (Tsai et al., 2011; Commenge et al., 2011; Hecht and Kraut, 2010; Constantinou and Gavrilidis, 2010; Atcharyawut et al., 2008; Liu et al., 2006; Park et al., 2005; Linek et al., 2001; Aroonwilas et al., 2001, 1999; Ji et al., 1999; Herskowitz et al., 1990; Svoboda and Rylek, 1979).

Recently, however, much research has been carried out with the purpose of CO₂ emission reduction. CO₂ capture using a packed bed with NaOH aqueous solution has been proposed, and the calculation of the energy balance in the system was reported (Bacocchi et al., 2006; Zeman, 2007). In addition, a study on CO₂ absorption with a spray-based contactor for capture was carried out, and the energy balance as well as the feasibility of the technique were reported (Stolaroff et al., 2008). Improvement of the absorption

* Corresponding author. Tel.: +82 2 2164 4866; fax: +82 2 2164 4765.
E-mail addresses: jhwee@catholic.ac.kr, jhwee@korea.ac.kr (J.-H. Wee).

capacity in a high-vortex spray scrubber was investigated (Javed and Mahmud, 2010).

Compared to MEA, NaOH (or in aqueous solution) cannot be readily regenerated because NaHCO_3 , the final product of CO_2 absorption to NaOH solution, is very soluble in aqueous solution. In addition, although NaHCO_3 is obtained as a precipitated powder, NaOH cannot easily be regenerated from it. This is primarily due to Na_2CO_3 . Whereas NaHCO_3 readily decomposes to Na_2CO_3 , H_2O and CO_2 at a relatively low temperature of about 160°C (Heda et al., 1995), Na_2CO_3 is thermally very stable and is decomposed to Na_2O , which is the direct source of NaOH, at very high temperatures over 800°C (Siriwardane et al., 2007).

However, extensive study has focused on the NaOH generation technology from Na_2CO_3 . The addition of $\text{Na}_2\text{O} \cdot 3\text{TiO}_2$ (Mahmoudkhani and Keith, 2009) or CaO (Siriwardane et al., 2007) to Na_2CO_3 significantly decreased the decomposition temperature of Na_2CO_3 . In addition, OH^- comprised materials such as $\text{Ca}(\text{OH})_2$ can be reacted with Na_2CO_3 to substitute OH^- for the CO_3^{2-} and thus recover NaOH (Bacocchi et al., 2006; Zeman, 2007; Stolaroff et al., 2008).

For applying the NaOH regeneration route via Na_2CO_3 , firstly, NaHCO_3 in the solution should be obtained as a powder during the absorption. Na_2CO_3 and NaHCO_3 powders can be obtained by absorbing CO_2 into NaOH aqueous solution via a spray dryer, as has been demonstrated in the literature (Chen et al., 2005; Stolaroff et al., 2008). Furthermore, the addition of CaO to NaOH aqueous solution enhances the CO_2 absorption in a spray dryer.

Therefore, if the NaOH generation issue is effectively addressed and considering the serious situation of climate change, CO_2 chemical absorption using NaOH aqueous solution has strong potential for application to CO_2 capture.

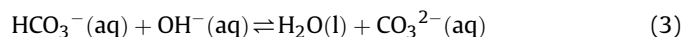
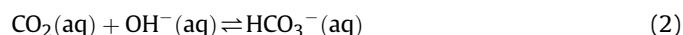
Therefore, the present paper investigates various features of NaOH aqueous solution as an absorbent for CO_2 capture. Firstly, to avoid the effect of CO_2 concentration in the flue gas on the absorption capacity of the solution, the CO_2 mole composition of the feeding gas mixture is maintained at a relatively high value of about 30% (balance N_2), which is similar to that of the cement and steel industries. Secondly, five kinds of NaOH aqueous solution are prepared and the absorption is carried out at ambient temperature and pressure in a batch reactor. From the experimental results, the absorption behavior is presented according to pH, absorption capacity, absorption time, rate and capture efficiency of the absorbents. A very detailed CO_2 absorption mechanism is proposed throughout the absorption reaction.

2. Theory

The mechanism of CO_2 absorption in NaOH aqueous solution can be explained as follows. Firstly, Na^+ and OH^- are almost completely ionized in pure water because NaOH is very strongly alkaline. Secondly, when gaseous CO_2 is fed into the NaOH solution to be absorbed, CO_2 is physically absorbed (Darmana et al., 2007) to aqueous CO_2 , as listed in Eq. (1).



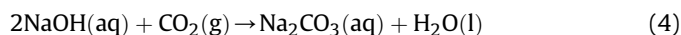
Subsequently, aqueous CO_2 reacts with OH^- to generate HCO_3^- and CO_3^{2-} , as expressed in Eqs. (2) and (3).



Although Eq. (2) is a second-order reaction, it can be considered a pseudo first-order reaction because the CO_2 concentration is

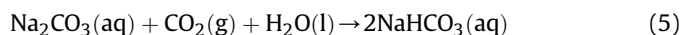
constant in the present work. Eqs. (2) and (3) are reversible reactions with very fast rates in high pH range (Fleischer et al., 1996). Reaction (3) is carried out immediately after reaction (2) (Guo et al., 2011). Aqueous CO_2 does not exist in the solution during the overall reaction because following its formation is immediately reacted with OH^- . Once aqueous CO_2 is generated in the solution, it is instantaneously consumed via reactions (2) and (3) (Fleischer et al., 1996).

Eq. (3) is dominant early in the reaction because the absorbent is maintained with a very high alkalinity, which further increases the CO_3^{2-} concentration relative to that of HCO_3^- (Fleischer et al., 1996). In addition, OH^- is rapidly decreased via reactions (2) and (3). Therefore, while pH is rapidly decreased during the initial reaction period, the CO_3^{2-} concentration is increased. Based on these phenomena, the net reaction carried out during the initial time (or range) of overall CO_2 absorption reaction is expressed as listed in Eq. (4).

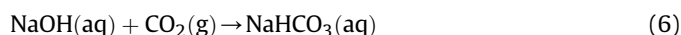


Although Na_2CO_3 is produced, it exists as dissociated Na^+ and CO_3^{2-} in the absorbent.

Subsequently, as CO_2 is continuously fed into the NaOH solution during the reaction, CO_2 is continuously absorbed, which leads to OH^- depletion and CO_3^{2-} accumulation via Eq. (2) and the forward reaction of (3). However, the CO_3^{2-} concentration increase causes the backward reaction of (3) to be more favored, which accelerates the forward reaction of (2). Therefore, the HCO_3^- concentration and pH are decreased in this range. The net reaction carried out in this second range of the overall absorption reaction can be expressed as Eq. (5)



After reaction (5) is completed at equilibrium, a slight amount of CO_2 may be additionally absorbed to make up for the shortage of physically unabsorbed CO_2 in water during the reaction. Finally, when NaOH is the limiting reactant, the overall CO_2 absorption reaction with NaOH in aqueous solution can be summarized as reaction (6), which is the net reaction of Eqs. (4) and (5).



3. Experimental and calculations

Five kinds of NaOH aqueous solution were prepared by dissolving granular NaOH powder (OCI, 99%) in 500 mL of distilled water. NaOH concentrations of the absorbent were in the range of 1wt.%–5wt.%. The absorption is presented schematically in Fig. 1.

A batch-typed Pyrex cylindrical reactor (D, 110 mm; h, 80 mm) equipped with a pH and electrical conductivity (EC) meter (Orion 4 Star, Thermo Scientific) was employed for the CO_2 absorption. Before absorption was conducted, the absorbent temperature was maintained at 25°C by a temperature controller and all equipment, including tubes, fittings and the empty space of the reactor, were sufficiently washed by N_2 purging. The CO_2 composition in the feed gas was maintained at approximately 31.5% by mixing with a N_2 balance in a gas mixer.

After the CO_2 composition and flow rate in the system were completely stabilized, the absorption was carried out by injecting the gas mixture into the absorbents via a sparger with a flow rate of 3 L/min controlled by a mass flow controller (MPR-2000, MKP). The stirrer was rotated at a speed of 180 rpm for uniform reaction in an absorber. The CO_2 composition in the outlet gas from the absorber

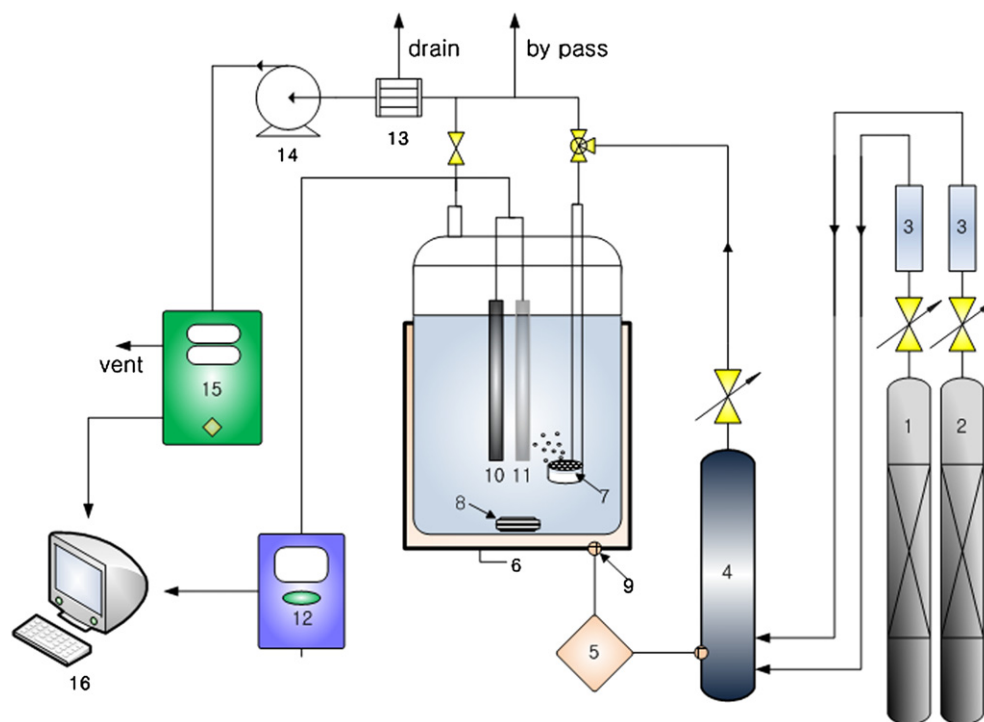


Fig. 1. Schematic of the CO₂ capture system using NaOH aqueous solution: (1) N₂ cylinder, (2) CO₂ cylinder, (3) Mass flow controller (MFC), (4) Gas mixer, (5) Temperature controller, (6) Pyrex Reactor, (7) Sparger, (8) Magnetic stirrer, (9) Thermometer, (10) pH sensor, (11) EC sensor, (12) pH/EC meter, (13) Dehumidifier, (14) Sampling pump, (15) Gas analyzer, and (16) Computer for data acquisition.

was measured every 1 s by using a non-dispersive infrared-based gas analyzer (maMos-200, Madur Electronics) and the variations of pH and EC during the reaction were measured every 5 s. These data were directly acquired by a computer for calculation. The amount of CO₂ absorbed in the absorbent was calculated based on the outlet CO₂ composition, gas flow rate and unchanged absolute amount of fed N₂ (Han et al., 2011).

The completion of the reaction was determined solely based on the point at which the outlet CO₂ composition was fully recovered to the initial value. Based on these measurements, the amount of CO₂ absorbed in the NaOH aqueous solution and the other involved values were calculated. Meanwhile, some substances that precipitated in the sparger during the absorption in the relatively highly concentrated NaOH solution were analyzed using X-ray diffraction (XRD; D5000, Siemens) and thermal gravimetric analysis (TGA; TGA2050, TA instruments, KBSI).

4. Results

4.1. CO₂ absorption behavior according to NaOH concentration

4.1.1. Absorption behavior in overall absorption range

When CO₂ was absorbed in 1, 3 and 5% NaOH solutions, Fig. 2 shows the variation of the outlet CO₂ composition, pH and EC during the overall reaction time.

Considering the pH variation and absorbed CO₂ amount, the overall reaction could be divided into 3 sections, as denoted in each figure. Reactions (4) and (5) were expected to be carried out in sections 1 and 2, respectively. Thereafter, the physical absorption of CO₂ was considered to have been favorably conducted in section 3.

When the CO₂ gas mixture was injected into the 1% NaOH solution, the absorption occurred instantaneously and the outlet CO₂ composition was sharply decreased to a minimum value within

16 s, as shown in Fig. 2(a). Subsequently, the outlet CO₂ composition was also sharply increased within a few seconds and gradually recovered to the initial value at the endpoint. Two inflexion points could be calculated by the time derivative of pH variation during the overall reaction. The first one was found at pH 10.91, which corresponded to the lowest EC. Therefore, the range between the initial point and the first inflexion point could be assumed to be section 1, in which reaction (4) was carried out. Thereafter, the pH was decreased to 7.7 for a relatively long time and the second inflexion point was indicated at this position. Therefore, the range between the two inflexion points was regarded as section 2. EC was little changed in this section, indicating that reaction (5) was dominant in section 2.

Although the same patterns were also exhibited in Fig. 2(b) and (c), the appearance of the inflexion points was further delayed and the EC level and pH at the inflexion points were higher than those of 1% NaOH solution due to their relatively high OH[−] concentration.

Finally, when the amount of absorbed CO₂, pH and EC variation were in-situ measured during the overall absorption reaction in each absorbent, as shown in Fig. 2, sufficient information on the absorption behavior was obtained, including the timing and extent of reactions (4) and (5) during the overall reaction. In addition, the in-situ concentration of every ion involved in absorption could be predicted. Consequently, the CO₂ absorption in the NaOH solution could be divided into three sections, as detailed below.

4.1.2. Absorption in individual reaction ranges

Fig. 3 shows the cumulative amount of CO₂ absorbed in 3 individual sections of 3% absorbents and the concentration variation of the involved ions that existed in the solution.

Na⁺ was not indicated in the figure because it is a spectator ion. Based on these data, the detailed reaction mechanism in each section was determined and is described below.

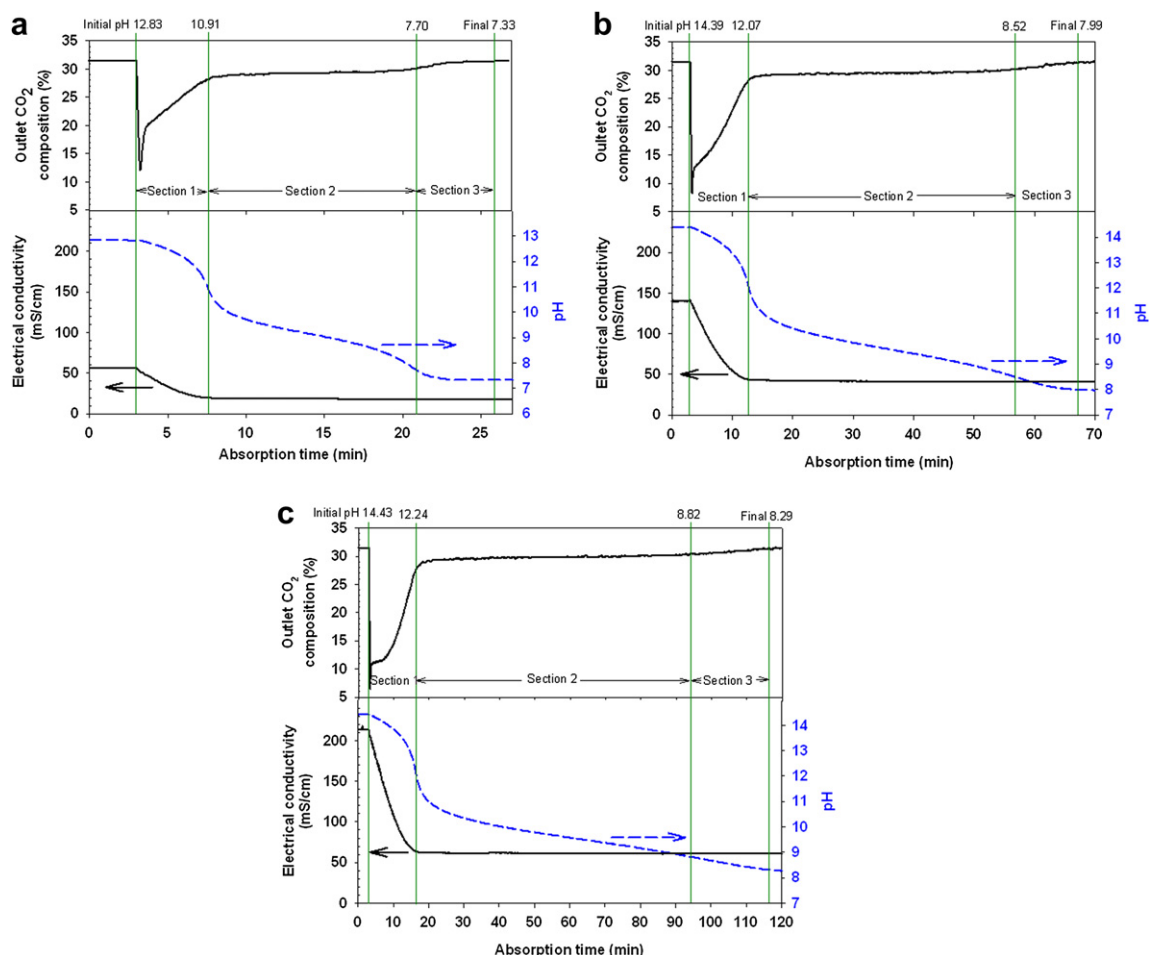


Fig. 2. Variation of outlet CO₂ composition, electrical conductivity (EC), and pH in (a) 1%, (b) 3% and (c) 5% NaOH solutions according to absorption time.

- Section 1: As the absorption started, reactions (1) and (2) commenced. Therefore, significant OH[−] was consumed to produce CO₃^{2−} and the pH was decreased in this section. EC was also significantly reduced in this section, which was ascribed to the fact that the equivalent EC of the depleted OH[−] (198.6 S cm²/mol z) was 3.6-fold larger than that of the generated CO₃^{2−} (55 S cm²/mol z). The EC decrease in this section was further evidence demonstrating that reaction (4) was primarily conducted in this section. Therefore, the largest amount of CO₂ was absorbed in this section with the highest reaction rate.
- Section 2: As reaction (4) was terminated and the alkalinity was decreased, the backward reaction of (3) and the forward reaction of (2) became dominant. Therefore, reaction (5) was further activated, which reduced the CO₃^{2−} concentration from the highest point and linearly increased the HCO₃[−] concentration to the second inflexion point, as shown in Fig. 3. Meanwhile, a very slight amount of H⁺ was dissociated from HCO₃[−], which decreased the pH in this section. However, EC was little changed in this section because of the similarity between the equivalent EC values of the consumed CO₃^{2−} and the generated HCO₃[−] (44.5 S cm²/mol z). H⁺ may have had little effect on the EC variation due to its relatively small amount in this section. Finally, while CO₂ was substantially absorbed in this section according to reaction (5), the absorption rate was less than that of section 1.
- Section 3: Following the second inflexion point, the OH[−] concentration was very low and the chemical absorption was almost finalized. Therefore, CO₂ was considered to have been physically absorbed as much as the equilibrium value in water at a given partial pressure. Furthermore, a slight amount of CO₂ may have been additionally absorbed due to some residual OH[−] in the enriched NaOH solution.

Table 1 summarizes the amount of CO₂ absorbed, yield (experimental value of CO₂ absorbed/theoretical value of CO₂ absorbed), NaOH utilization (g of CO₂ chemically absorbed/g of NaOH in solution) and specific CO₂ capture capacity (mg of total CO₂ absorbed/g of NaOH solution) for each absorbent.

Table 1 reveals that the previously mentioned absorption behavior in each section was valid. For example, the theoretical amount of CO₂ absorbed to calculate the yield in sections 1 and 2 was based on reactions (4) and (5), respectively. All measured values in Table 1 were determined with considerations for the error of measuring equipment. The yield of every absorbent was nearly one, indicating that reactions (4) and (5) were primarily carried out in sections 1 and 2, respectively. However, every yield was very slightly deviated from one. Furthermore, the NaOH utilization of every absorbent, excluding the CO₂ physical absorption, was slightly less than 1.1, which is the stoichiometric utilization of the absorbent according to reaction (6). These slight deviations were ascribed to the fact that the CO₂ physical absorption in each section

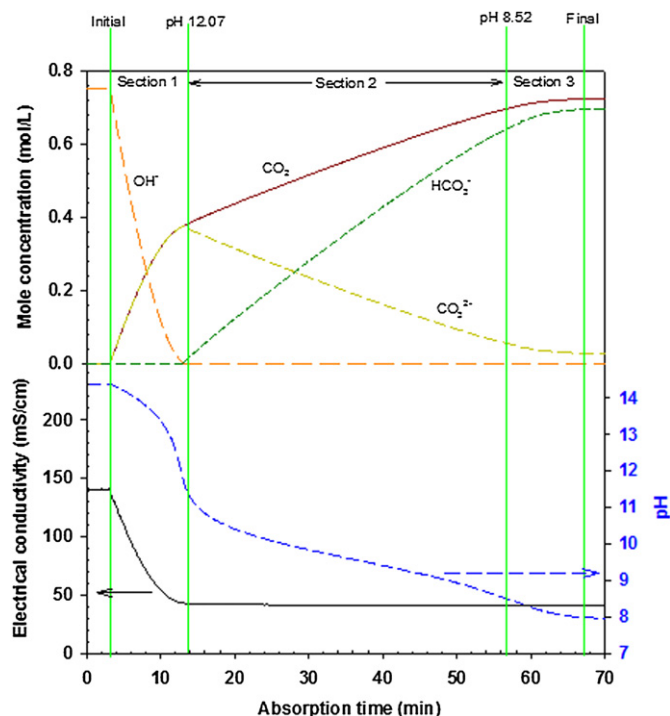


Fig. 3. Concentration variation of absorbed CO_2 and existing ions in each reaction section of 3% NaOH solution according to absorption time.

was slightly different from the absorbents and the possible involvement of a side reaction of (6). Although the utilization and specific capture capacity of the 2% NaOH solution were slightly higher than those of other solutions, the differences were negligible. Therefore, the specific CO_2 capture capacity in NaOH aqueous solution of approximately 2 mg of CO_2 per g of NaOH and g of water was independent of the NaOH concentration. Therefore, an enriched NaOH solution may be more effectively used as the absorbent in terms of total CO_2 absorption capacity of the solution.

4.1.3. Absorption rate and CO_2 capture efficiency

The absorption capacity and rate of each absorbent are shown in Fig. 4.

The slope in Fig. 4(a) is the absorption rate: two different rates were calculated for every absorbent. The first, which was larger than the second, was the absorption rate in section 1, which was proportional to the NaOH concentration, as shown in Fig. 4(b). Therefore, reaction (4) can be considered a first-order reaction solely dependent on the OH^- concentration. Therefore, the CO_2 capture efficiency in section 1 according to the absorbent was proportional to the OH^- concentration and was about 50% for 3% NaOH solution, as listed in Table 2.

On the other hand, the second slope, which indicates the reaction rate in section 2, was very small compared to first one. The

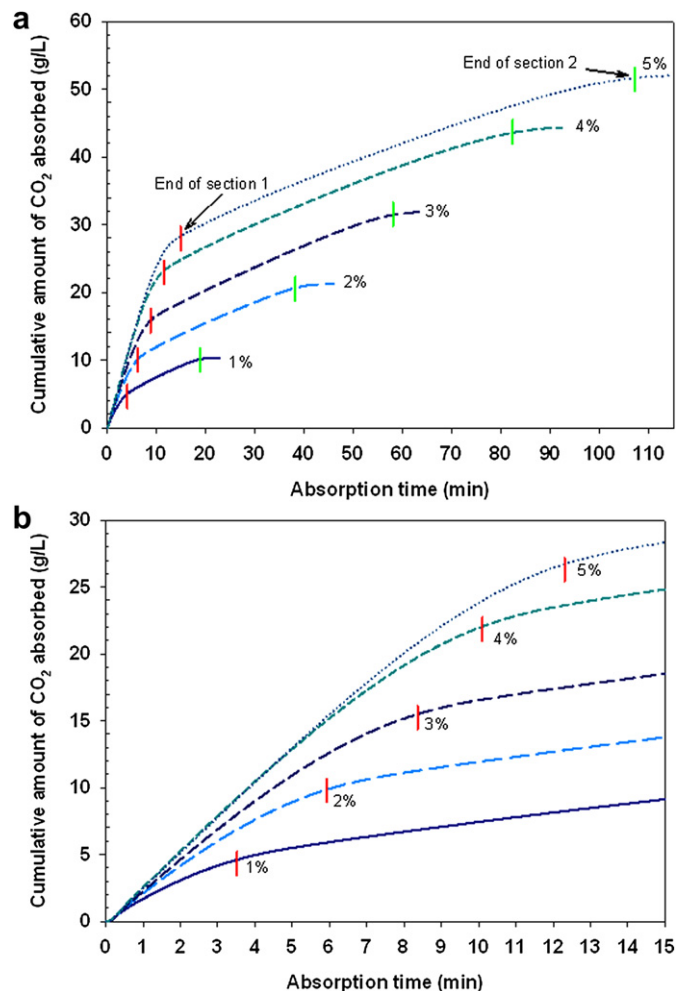


Fig. 4. Cumulative amount of CO_2 absorbed and absorption rate in each concentration during (a) the overall reaction time, (b) the reaction time of section 1.

slopes in all absorbents were almost the same, as shown in Fig. 4(a). This indicated that the absorption conducted in section 2 was a zero-order reaction, i.e., it was independent of the CO_3^{2-} concentration. Therefore, the CO_2 capture efficiency in section 2 was approximately 9% for all absorbents.

4.2. CO_2 absorption capacity of absorbents

4.2.1. Variation of CO_2 composition and total amount of CO_2 absorbed

The in-situ variations of the outlet CO_2 composition in the gas mixture that passed each absorbent are shown in Fig. 5.

Table 1
Amount of CO_2 absorbed, yield, NaOH utilization and capture capacity in each section of the absorbents.

Individual reaction range		NaOH solution concentration				
		1%	2%	3%	4%	5%
Section 1	Amount of CO_2 absorbed (g)	2.6443	5.3956	8.1867	10.9005	13.7185
	Yield	0.9616	0.9810	0.9923	0.9910	0.9977
Section 2	Amount of CO_2 absorbed (g)	2.3334	4.9212	7.1302	9.6740	11.0128
	Yield	0.9935	1.0477	1.0120	0.8442	0.9378
Section 3	Amount of CO_2 absorbed (g)	0.1805	0.3007	0.5804	0.7658	1.2843
Utilization		0.9955	1.0317	1.0211	1.0287	0.0983
Specific CO_2 capture capacity		2.0632	2.2134	2.1300	2.0952	2.0812

Table 2
CO₂ capture efficiency of the absorbents in each section.

NaOH solution concentration	CO ₂ capture efficiency (%)	
	Section 1	Section 2
1%	35.73	10.84
2%	43.05	9.31
3%	48.88	9.37
4%	52.44	9.67
5%	57.99	8.01

The recovery time from the CO₂ outlet composition to the initial CO₂ composition was linearly delayed according to the NaOH concentration. The CO₂ absorption capacity of the absorbent was calculated by integrating the area enclosed by each line in Fig. 5. The calculated CO₂ absorption capacity of each absorbent, including 0.52 g of CO₂, which is the amount of CO₂ absorbed in pure water, is shown as 5 dots in Fig. 6. The absorption capacity was positively correlated with the NaOH concentration.

Meanwhile, when the overall reaction of CO₂ with NaOH in solution was carried out solely based on reaction (6), the theoretical amount of CO₂ absorbed in each absorbent, including 0.52 g of CO₂, and is shown as a solid line in Fig. 7.

The experimental value of CO₂ absorption capacity in each absorbent was slightly smaller than the theoretical value and its difference increased slightly with increasing NaOH concentration. Therefore, other minor reactions (or products) were expected to be involved in the CO₂ absorption, as is discussed in the next section.

4.2.2. Trona production

The solubility of NaHCO₃, the final product of reaction (6), was so high that it could not be obtained as precipitated powder in the reactor after the reaction completion in every absorbent. However, a slight amount of NaHCO₃ (or other mixed) powder could be obtained in a sparger after the absorption was completed with a relatively enriched NaOH solution such as the 4% and 5% absorbents. This result was ascribed to the fact that the sparger may have acted as the local reactor in which the NaHCO₃ supersaturated condition was instantaneously maintained due to the high NaOH concentration. If the reaction in the sparger was assumed to represent the overall reaction in a Pyrex reactor, analysis of the powder can provide detailed and crucial information on the absorption reactions, including reaction (6). Therefore, the powder

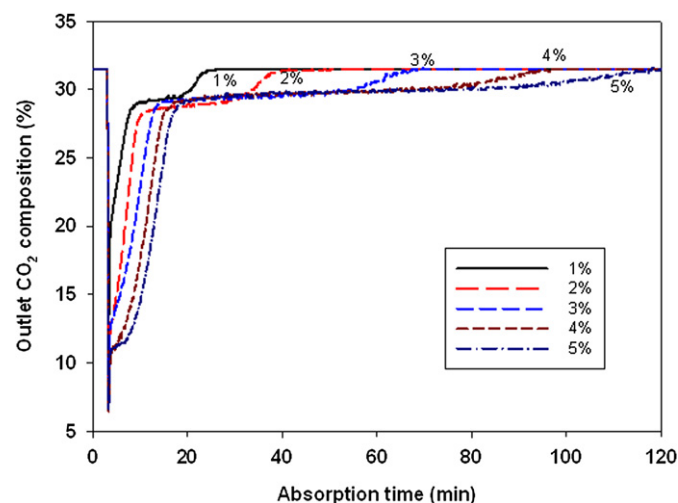


Fig. 5. Absorption behavior of CO₂ in each NaOH solution according to absorption time.

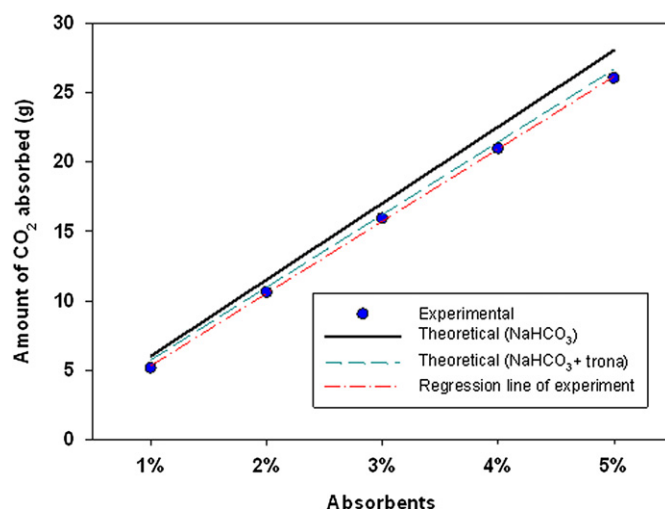
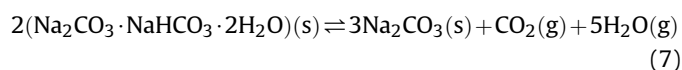


Fig. 6. Comparison of theoretical and experimental amounts of CO₂ absorbed in each NaOH solution.

was qualitatively and quantitatively analyzed using XRD and TGA. The results for the powder produced in 4% solution are shown in Figs. 7 and 8.

The XRD peaks show that the primary substance in the powder was NaHCO₃, with a slight amount of tri-sodium hydrogen-dicarbonate dihydrate (Na₂CO₃·NaHCO₃·2H₂O; trona) mixed in the powder.

Further evidence of slight trona presence in the powder was confirmed by TGA analysis. Fig. 8(b) was substantially different from Fig. 8(a), which is the TGA data of pure NaHCO₃. The first weight loss of the powder, approximately 4%, was indicated at about 100 °C, as shown in Fig. 8(b). This was attributed to the thermal decomposition of trona to H₂O and CO₂, as listed in Eq. (7) (Ekmekyapar et al., 1996; Liu and Fleet, 2009).



The second weight loss at 150 °C was due to thermal decomposition of NaHCO₃, as listed in reaction (8), which is the reversible reaction of (5) (Ekmekyapar et al., 1996; Liu and Fleet, 2009).

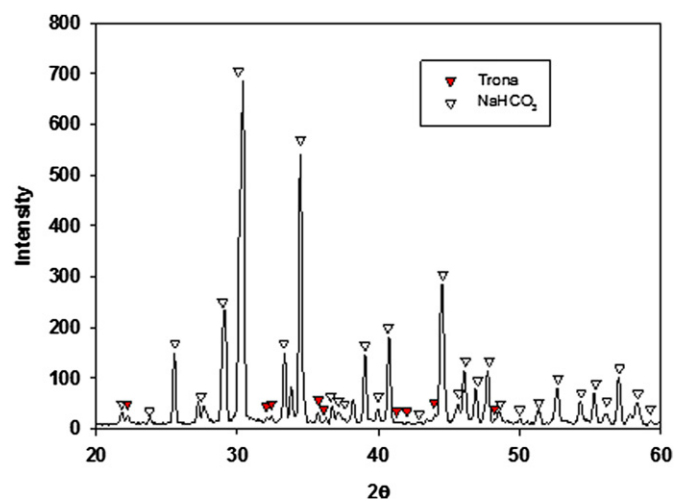


Fig. 7. X-ray diffraction (XRD) patterns of the precipitated powder produced in 4% NaOH solution.

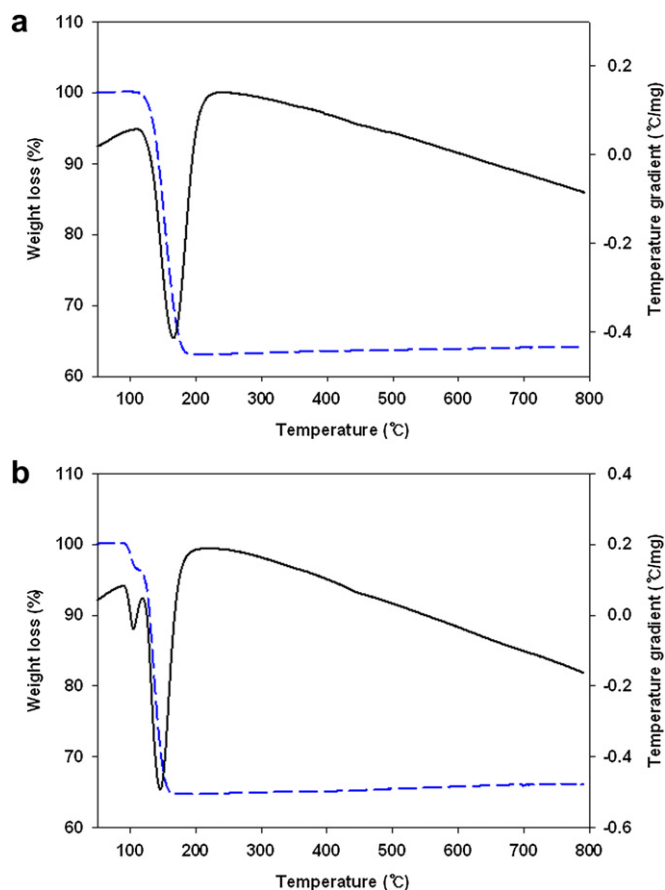
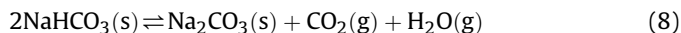


Fig. 8. Thermal gravimetric analysis (TGA) patterns of (a) pure NaHCO_3 and (b) the precipitated powder produced in 4% NaOH solution.



5. Conclusion

The present paper has investigated the various features of NaOH aqueous solution to capture CO_2 at relatively high CO_2 composition in the gas mixture. The features included CO_2 absorption capacity, rate, capture efficiency and detailed absorption mechanism. The following conclusions were derived from the experiment and data analysis.

- Considering the variation in pH, EC and amount of absorbed CO_2 in the solution, the overall CO_2 absorption reaction was carried out in three consecutive steps. Reactions (4) and (5) primarily occurred in the reactions of sections 1 and 2, respectively. Thereafter, physical absorption dominated in section 3.
- The utilization of NaOH solution to capture CO_2 almost reached the theoretical value and was not dependent on the NaOH concentration. However, the absorption rate was proportional to the NaOH concentration. Therefore, enriched NaOH solution can be more effectively used as the absorbent in terms of the total CO_2 absorption capacity and rate.
- Reaction (4) was a first-order reaction solely dependent on the OH^- concentration and the CO_2 capture efficiency significantly increased to 57% with the 5% NaOH solution. However, the reaction rate of (5) in section 2 was almost independent of the CO_3^{2-} concentration and the CO_2 capture efficiency in this section was approximately 10% for all absorbents.

- The backward reaction of (7) contributed slightly to CO_2 absorption in the NaOH aqueous solution, which resulted in trona production. Based on the experimental data and estimations, the mass ratio of CO_2 absorbed for Na_2CO_3 , NaHCO_3 , and trona production was calculated to be 20:17:1, respectively. This was confirmed by identifying the experimental and theoretical values of CO_2 absorbed.

Acknowledgments

This research was supported by Basic Research Program through the National Research Foundation of Korea (NRF) funded by the Ministry of Education, Science and Technology (2010-0009938) as well as supported by the Catholic University of Korea, Research Fund, 2011.

References

- Aroonwilas, A., Veawab, A., Tontiwachwuthikul, P., 1999. Behavior of the mass-transfer coefficient of structured packings in CO_2 absorbers with chemical reactions. *Ind. Eng. Chem. Res.* 38, 2044–2050.
- Aroonwilas, A., Tontiwachwuthikul, P., Chakma, A., 2001. Effects of operating and design parameters on CO_2 absorption in columns with structured packings. *Sep. Purif. Technol.* 24, 403–411.
- Atchariyawut, S., Jiratananon, R., Wang, R., 2008. Mass transfer study and modeling of gas-liquid membrane contacting process by multistage cascade model for CO_2 absorption. *Sep. Purif. Technol.* 63, 15–22.
- Bacocchi, R., Storti, G., Mazzotti, M., 2006. Process design and energy requirement for the capture of carbon dioxide from air. *Chem. Eng. Process.* 45, 1047–1058.
- Chen, J.-C., Fang, G.-C., Tang, J.-T., Liu, L.-P., 2005. Removal of carbon dioxide by a spray dryer. *Chemosphere* 59, 99–105.
- Commenge, J.-M., Obein, T., Framboisier, X., Rode, S., Pitiot, P., Matlosz, M., 2011. Gas-phase mass-transfer measurements in a falling-film microreactor. *Chem. Eng. Sci.* 66, 1212–1218.
- Constantinou, A., Gavrilidis, A., 2010. CO_2 absorption in a microstructured mesh reactor. *Ind. Eng. Chem. Res.* 49, 1041–1049.
- Darmana, D., Henket, R.L.B., Deen, N.G., Kuipers, J.A.M., 2007. Detailed modelling of hydrodynamics, mass transfer and chemical reactions in a bubble column using a discrete bubble model: chemisorption of CO_2 into NaOH solution, numerical and experimental study. *Chem. Eng. Sci.* 62, 2556–2575.
- Ekmekyapar, A., Ersuahan, H., Yapici, S., 1996. Nonisothermal decomposition kinetics of trona. *Ind. Eng. Chem. Res.* 35, 258–262.
- Fleischer, C., Becker, S., Eigenberger, G., 1996. Detailed modeling of the chemisorptions of CO_2 into NaOH in a bubble column. *Chem. Eng. Sci.* 51, 1715–1724.
- Gangopadhyay, P.K., Van der Meer, F., Van Dijk, P., 2008. Atmospheric modelling using FASCOD to identify CO_2 absorption bands and their suitability analysis in variable concentrations for remote sensing applications. *J. Quant. Spectrosc. Radiat. Transf.* 109, 670–683.
- Gerard, D., Wilson, E.J., 2009. Environmental bonds and the challenge of long-term carbon sequestration. *J. Environ. Manage.* 90, 1097–1105.
- Guo, Y., Niu, Z., Lin, W., 2011. Comparison of removal efficiencies of carbon dioxide between aqueous ammonia and NaOH solution in a fine spray column. *Energy Procedia* 4, 512–518.
- Han, S.-J., Yoo, M., Kim, D.W., Wee, J.-H., 2011. Carbon dioxide capture using calcium hydroxide aqueous solution as the absorbent. *Energy Fuels* 25, 3825–3834.
- Hecht, K., Kraut, M., 2010. Thermographic investigations of a microstructured thin film reactor for gas/liquid contacting. *Ind. Eng. Chem. Res.* 49, 10889–10896.
- Heda, P.K., Dollimore, D., Alexander, K.S., Chen, D., Law, E., Bicknell, P., 1995. A method of assessing solid state reactivity illustrated by thermal decomposition experiments on sodium bicarbonate. *Thermochim. Acta* 225, 255–272.
- Heitmann, N., Khalilian, S., 2011. Accounting for carbon dioxide emissions from international shipping: burden sharing under different UNFCCC allocation options and regime scenarios. *Mar. Policy* 35, 682–691.
- Herskowitz, D., Herskowitz, V., Stephan, K., Tamir, A., 1990. Characterization of a two-phase impinging jet absorber-II. Absorption with chemical reaction of CO_2 in NaOH solutions. *Chem. Eng. Sci.* 45, 1281–1287.
- Javed, K.H., Mahmud, E.P., 2010. The CO_2 capture performance of a high-intensity vortex spray scrubber. *Chem. Eng. J.* 162, 448–456.
- Ji, X., Kritiphat, W., Aboudheir, A., Tontiwachwuthikul, P., 1999. Mass transfer parameter estimation using optimization technique: case study in CO_2 absorption with chemical reaction. *Can. J. Chem. Eng.* 77, 69–73.
- Kittel, J., Idem, R., Gelowitz, D., Tontiwachwuthikul, P., Parrain, G., Bonneau, A., 2009. Corrosion in MEA units for CO_2 capture: pilot plant studies. *Energy Procedia* 1, 791–797.
- Leifsen, H., 2007. Post-combustion CO_2 Capture Using Chemical Absorption. Norwegian University of Science and Technology (Master thesis), Trondheim, 9 pp.

- Linek, V., Moucha, T., Rejl, F.J., 2001. Hydraulic and mass transfer characteristics of packings for absorption and distillation columns. *Rauschert-Metall-Sattel-Rings*. *Chem. Eng. Res. Des.* 79, 725–732.
- Liu, X., Fleet, M.E., 2009. Phase relations of nahcolite and trona at high P-T conditions. *J. Miner. Petrol. Sci.* 104, 25–36.
- Liu, G.B., Yu, K.T., Yuan, X.G., Liu, C.J., 2006. New model for turbulent mass transfer and its application to the simulations of a pilot-scale randomly packed column for CO₂-NaOH chemical absorption. *Ind. Eng. Chem. Res.* 45, 3220–3229.
- Mahmoudkhani, M., Keith, D.W., 2009. Low-energy sodium hydroxide recovery for CO₂ capture from atmospheric air – thermodynamic analysis. *Int. J. Greenhouse Gas Control* 3, 376–384.
- Nguyen, T., Hilliard, M., Rochelle, G.T., 2010. Amine volatility in CO₂ capture. *Int. J. Greenhouse Gas Control* 4, 707–715.
- Park, S.-W., Choi, B.-S., Lee, B.-D., Lee, J.-W., 2005. Chemical absorption of carbon dioxide into aqueous PAA solution of NaOH. *Separ. Sci. Technol.* 40, 911–926.
- Qin, F., Wang, S., Hartono, A., Svendsen, H.F., Chen, C., 2010. Kinetics of CO₂ absorption in aqueous ammonia solution. *Int. J. Greenhouse Gas Control* 4, 729–738.
- Siriwardane, R.V., Robinson, C., Shen, M., Simonyi, T., 2007. Novel regenerable sodium-based sorbents for CO₂ capture at warm gas temperatures. *Energy Fuels* 21, 2088–2097.
- Spector, N.A., Dodge, B.F., 1946. Removal of carbon dioxide from atmospheric air. *Trans. Am. Inst. Chem. Eng.* 42, 827–848.
- Stolaroff, J.K., Keith, D.W., Lowry, G.V., 2008. Carbon dioxide capture from atmospheric air using hydroxide spray. *Environ. Sci. Technol.* 42, 2728–2735.
- Svoboda, K., Rylek, M., 1979. Measurement of interfacial area and mass transfer coefficients by chemical method of CO₂ absorption into aqueous solutions of NaOH in a model column with expanded metal sheet packing. *Chem. Eng. Commun.* 3, 399–411.
- Tepe, J.B., Dodge, B.F., 1943. Absorption of carbon dioxide by sodium hydroxide solutions in a packed column. *Trans. Am. Inst. Chem. Eng.* 39, 255–276.
- Tsai, R.E., Seibert, A.F., Eldridge, R.B., Rochelle, G.T., 2011. A dimensionless model for predicting the mass-transfer area of structured packing. *AIChE J.* 57, 1173–1184.
- Zeman, F., 2007. Energy and material balance of CO₂ capture from ambient air. *Environ. Sci. Technol.* 41, 7558–7563.
- Zhao, X.-Y., Qian, J.-L., Wang, J., HE, Q.-Y., Wang, Z.-L., Chen, C.-Z., 2006. Using a tree ring S13C annual series to reconstruct atmospheric CO₂ concentration over the past 300 Years. *Soil Sci. Soc. China* 16, 371–379.
- Zhao, B., Sun, Y., Yuan, Y., Gao, J., Wang, S., Zhuo, Y., Chen, C., 2011. Study on corrosion in CO₂ chemical absorption process using Amine solution. *Energy Procedia* 4, 93–100.